AD-A040 256 LARGE CALIBER WEAPON SYSTEMS LAB (ARMY) DOVER N J F/G 17/5
A PRELIMINARY THERMOGRAPHIC HEAT SURVEY OF ARRADCOM FACILITIES --ETC(U)
APR 77 P KISATSKY, M BARBARISI, G TIRELLIS
UNCLASSIFIED ARLCD-TR-77014 NL

ADA040256

12

AD

COPY NO. 10

TECHNICAL REPORT ARLCD-TR-77014

A PRELIMINARY THERMOGRAPHIC HEAT SURVEY OF ARRADCOM FACILITIES (DOVER, NJ)

PAUL KISATSKY
MODESTO BARBARISI
GUS TIRELLIS

APRIL 1977

US ARMY ARMAMENT RESEARCH AND DEVELOPMENT COMMAND
LARGE CALIBER
WEAPON SYSTEMS LABORATORY
DOVER, NEW JERSEY

APPROVED FOR PUBLIC RELEASE; DISTRIBUTION UNLIMITED.

The findings in this report are not to be construed as an official Department of the Army position.

DISPOSITION

Destroy this report when no longer needed. Do not return to the originator.

UNCLASSIFIED (14)

SECURITY CLASSIFICATION OF THIS PAGE (When Data Entered)

REPORT DOCUMENTATION PAGE

READ INSTRUCTIONS BEFORE COMPLETING FORM

1. REPORT NUMBER
(9) Technical Report, ARLCD-TR-77014

2. GOVT ACCESSION NO.

3. RECIPIENT'S CATALOG NUMBER

4. TITLE (and Subtitle)
(6) A PRELIMINARY THERMOGRAPHIC HEAT SURVEY OF ARRADCOM FACILITIES (DOVER, NJ).

5. TYPE OF REPORT & PERIOD COVERED

6. PERFORMING ORG. REPORT NUMBER

7. AUTHOR(s)
(10) Paul/Kisatsky,
Modesto/Barbarisi
Gus/Tirellis

8. CONTRACT OR GRANT NUMBER(s)

9. PERFORMING ORGANIZATION NAME AND ADDRESS
Engineering Sciences Division, FRL
Picatinny Arsenal
Dover, NJ 07801

10. PROGRAM ELEMENT, PROJECT, TASK AREA & WORK UNIT NUMBERS
(12) 43p.

11. CONTROLLING OFFICE NAME AND ADDRESS
ARRADCOM, LCWSL
Applied Sciences Division (DRDAR-LCA)
Dover, NJ 07801

12. REPORT DATE
(11) Apr[redacted]77

13. NUMBER OF PAGES
48

14. MONITORING AGENCY NAME & ADDRESS (if different from Controlling Office)

15. SECURITY CLASS. (of this report)
Unclassified

15a. DECLASSIFICATION/DOWNGRADING SCHEDULE

16. DISTRIBUTION STATEMENT (of this Report)

Approved for public release, distribution unlimited.

17. DISTRIBUTION STATEMENT (of the abstract entered in Block 20, if different from Report)

18. SUPPLEMENTARY NOTES

19. KEY WORDS (Continue on reverse side if necessary and identify by block number)

Thermography	Heat transfer
Infrared	Insulation
Energy conservation	Heat conservation

20. ABSTRACT (Continue on reverse side if necessary and identify by block number)

An infrared thermographic survey was made of buildings and facilities in Picatinny Arsenal. The purpose of the survey was to demonstrate the usefulness of IR thermography as a diagnostic technique to discover and identify sources of heat loss. Several examples are shown in which thermography yields valuable information on insulation deficiencies, poorly insulated steam lines, running vent fans, open windows, etc. It is shown

→ next page

DD FORM 1 JAN 73 1473 EDITION OF 1 NOV 65 IS OBSOLETE

UNCLASSIFIED

SECURITY CLASSIFICATION OF THIS PAGE (When Data Entered)

410 163

mt

UNCLASSIFIED

SECURITY CLASSIFICATION OF THIS PAGE(When Data Entered)

20. ABSTRACT (Continued)

cont.

that thermographic data needs careful interpretation and is vulnerable to emissivity variations. Parameters for developing a quantitative thermographic methodology are identified as a basis for future work.

UNCLASSIFIED

SECURITY CLASSIFICATION OF THIS PAGE(When Data Entered)

ACKNOWLEDGMENT

To Bill Doremus and John Gregorits, our supervision, whose continuing support of our efforts is based on their firm belief that creativity is the mainspring of the new technology required to meet Army needs of tomorrow. To Jack Swotinsky and Chip Morrow, who encouraged that this type of effort be initiated and sustained so that we can learn to apply new technology to Army production problems of today.

To Product Assurance Directorate, PTA for lending us our first set of thermographic instrumentation. Last but not least, to Earl Paulison, ISSD, whose van will never be the same after the banging and battering experience it received during our tests.

TABLE OF CONTENTS

SUMMARY

In response to interest shown in the use of IR imaging for energy conservation purposes, a preliminary thermographic survey was made of various Picatinny Arsenal buildings and facilities during the winter of 1976. The thermograms display qualitative information and demonstrate the categories of observable phenomena when employing this technique. The basic principles of IR thermography are discussed and the major pitfalls of "qualitative" thermography are pointed out. Prior to relating IR imagery to actual heat losses, it is necessary to determine actual surface temperatures in contrast to radiometric temperature. Great care must be exercised in correcting for emissivity variations and reflected radiance components. The interplay of conduction, convection and radiation dictate actual heat loss and these factors must be considered in order not to draw erroneous conclusions. Development of a methodology to measure true surface temperatures and relate them to a quantitative heat transfer model is necessary and will be a goal of further work in this technology.

INTRODUCTION

Prior to the winter of 1974-1975, the Engineering Sciences Division proposed the utilization of modern thermographic imaging techniques as a useful diagnostic method to apply to problems relating to the energy crisis. As suggested in the original proposal (ESD Information Report No. 624), thermographic data could be useful for fuel conservation efforts either from the viewpoint of heat losses from external industrial facilities (i.e., buildings, steam lines, etc) or to internal plant process studies as for chemical/explosive production lines.

As a consequence of the proposed work, two areas of interest were aroused at Picatinny Arsenal. Facilities personnel were interested in such things as adequacy of insulation and its relationship to heat loss in winter, while manufacturing technology personnel felt this would be an applicable technique to assist in conducting heat balance inventories in explosive production. Such studies are considered vital to energy conservation in manufacturing.

Accordingly, the Engineering Sciences Division conducted a small effort in acquiring thermal images of various arsenal facilities. This was done both to demonstrate the usefulness of the method, as well as to acquire a better feel for its limitations. We further hoped to define what methodology need be developed to turn the technique from a qualitative demonstration into a meaningful and practical method with measurable payoff in fuel/dollar savings. Taking advantage of the time of the year, first emphasis was placed on looking at exterior facilities. Efforts to thermograph a typical interior of an explosive "meltpour" pilot plant, were initiated and is being continued.

BACKGROUND PRINCIPLES OF THERMOGRAPHY

It is well known from basic physics that all objects at a finite temperature radiate energy. The quantity and quality of this radiated power has been thoroughly investigated and its description is embodied in Planck's Radiation Formula. (Appendix) Planck's Law is strictly valid for blackbodies which are perfect radiators, but it also serves to account for the radiation emitted by any real surface if we take into account the "emissivity" of the surface. Emissivity is a measure of the relative ease with which a surface can radiate and is expressed as a fraction of that which a perfect radiator

(blackbody) would emit at the same temperature. Emissivity is, in turn, dependent both on the material in question as well as the physical condition of its surface (i.e., polished, rough, porous, etc). By carefully studying Planck's Law, quantitative determinations can be made as to how the radiant power depends on wavelength, surface temperature, and emissivity. As further shown in the appendix, the total amount of power radiated per unit surface area, for all wavelengths, increases with the fourth power of the absolute temperature.

For bodies at, or near, ambient temperatures, most of the emitted radiation takes place in the infrared (IR) region of the spectrum, peaking at about 10 microns. The radiation actually occupies a wide band, being significant from 3 microns to 40 microns. As a body heats up to higher temperature, the amount of radiation as well as its spectral distribution changes so that at higher temperatures a body radiates increasingly at shorter wavelengths tending toward the visible part of the spectrum.

Since our eyes are not sensitive to IR radiation, bodies at normal temperatures are invisible in the dark unless heated up to the point where they glow in the visible. A sensor which is sensitive to the IR will respond to the natural radiant emissions of warm bodies, and the received signal will increase (non-linearly) as the temperature increases. This is the fundamental mechanism of all thermographic imaging cameras.

The basic principle of a thermographic imaging system is shown in Figure 1. The performance of such a device is similar in many respects to a television camera. A lens of IR transmitting material (i.e., silicon) forms an IR image of the object onto a focal plate, not unlike an ordinary camera. Since film is not sensitive to the middle and a IR wavelength, it is necessary to employ a small, IR sensitive photocell. By a system of rotating mirrors, the image is caused to scan across the sensor in a horizontal and vertical raster scan similar to that of television. The resulting signal from the detector constitutes a video input for a cathode ray display tube. A real time, visible, television like display of the IR image of the scene is the result.

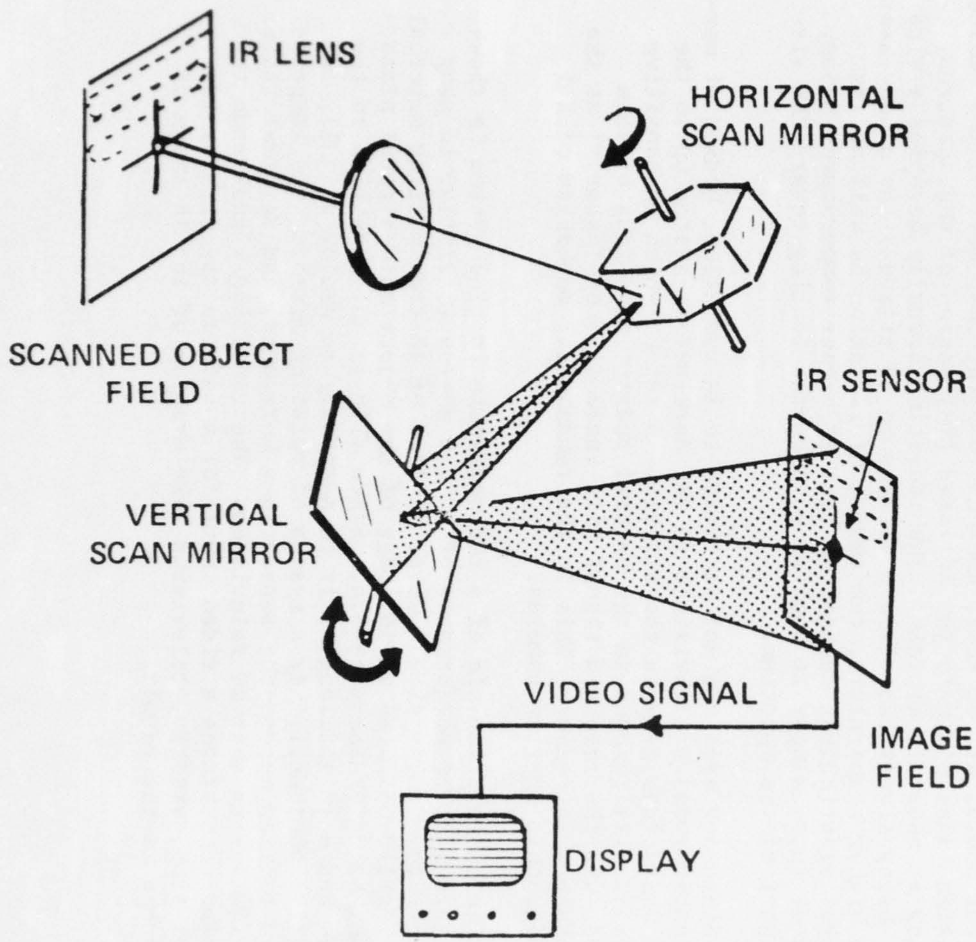

Fig 1 Basic infrared camera

DESCRIPTION OF EXPERIMENTS AND APPARATUS

Two types of commercial IR thermographic equipment were experimented with but the majority of the data in this report was taken with an AGA 680 system. The equipment was operated from a small van and powered with a gasoline generator which provided equipment compatible power. The data was taken at night between the hours of 1100 and 0600. This not only resulted in the elimination of solar confusion, but provided maximum contrasts resulting from the "warm" buildings against the cool night backgrounds. The camera was operated real time as the van was driven about random areas of Picatinny Arsenal. When areas of interest were spotted, the van was stopped for more intense scrutiny and photographs were taken as required. The thermograms were taken over several nights during which time the average outdoor air temperature ranged from -7°C (20°F) to 2°C (35°F).

The AGA equipment employs a cryogenically cooled, indium antimonide, photovoltaic detector sensitive to the spectral range of 2 to 5.6 microns. The electro-mechanical scanning arrangement provides a display of sixteen (16) frames per second with a raster scan of one hundred forty (140) standard TV lines of resolution. The instantaneous angular resolution of the system is 2.5 mrad for the standard FOV lens (25° x 25°) but is improved to 1.3 mrad for the telephoto (8° x 8°) lens. Most of the thermograms taken from ground level used the standard FOV lens.

In order to obtain the equivalent of aerial coverage, advantage was taken of the fact that much of Picatinny Arsenal lies in a valley and is observable from lookout points in the surrounding mountains. For these cases, a telephoto lens was employed and several thermograms were taken looking down at large portions of the arsenal.

In the resulting pictorial data, variations of object brightness (radiometric temperature) are seen as gray scale variations in the display. In order to remove subjectivity and to provide quantitative data, the technique of "isotherm contouring" was used as described here. When it is desired to estimate the actual radiometric temperature of a point in the scene, the instrument is used in the contouring mode. In this mode, a given threshold is set into the instrument, and all points at that particular signal level are displayed as bright points on the screen. The complete map of all these points therefore represent the isothermal contours of the scene. In effect, all regions at the same radiometric temperature become outlined. Two isotherms are actually used to estimate temperature. First, a suitable known background is chosen (such as

earth) as a reference temperature and is thermally contoured. A second isotherm is then chosen to map out all points at a given temperature increment above or below the reference temperature. When the point of interest falls in the isotherm contour of the second band, it is a simple matter to read the spacing of the two contour lines in "isotherm units." This reading does not represent the actual radiometric temperature separation due to the intrinsic nonlinearity of instrument signal response versus temperature. Isotherm units are numerically equivalent to temperature only over a small, linear portion of the instrument response which lies between 20°C to 40°C. For temperatures outside of this range it is necessary to interpret radiometric object temperature by appropriate use of calibration curves.

It is again emphasized here that the instrument measures radiometric temperature in contrast to true temperature. This is due to the fact that true temperature can differ from apparent, radiometric temperature because of emissivity variations in the object. This is discussed further in the "Technical Discussion/Problem Areas" portion of this report.

RESULTS OF INITIAL SURVEY

In this section we will describe the results obtained from the first thermographic survey. This survey was by no means complete nor was it intended to be so, but rather an initial indication of what practical results are obtained when this technology is applied to typical structures and heat generating components. A variety of objects were chosen for this initial survey including buildings, steamlines, electrical transformers, distribution junctions, and various other items which during the course of the survey caught our interest. This section will show many of the thermograms taken and in some cases a polaroid picture of the same structure taken during the daylight hours for comparison of structure detail. The explanation of each picture is intended to point out areas of interest. The interpretation is as accurate as possible at this stage but one must keep in mind that it is necessary to develop a complete methodology which includes variations in emissivity, reflectance, and other pertinent facts to yield a more accurate and complete analysis of the data.

Figure 2a is a thermographic display of the main entrance to the BOQ located on Navy Hill. The obvious places of heat loss such as windows and air vents, are indicated by their bright thermographic image. The areas of the building which the thermograph indicates as regions of heat loss which would not be otherwise obvious are the wall sections showing bright areas. These bright regions are warmer on the exterior of the building than the darker regions. The reason for this variation in outside wall temperature can be either poor insulations in these bright regions, or warmer temperature at the corresponding inside regions, such as the location of a radiator in the near proximity of the wall. In either case the addition of insulation or a reflecting material behind a radiator would decrease the amount of heat leaking through the outside wall surface.

Figure 3a shows the north end of building 183. As can be seen from this thermogram, the outside wall temperature appears quite uniform. The four windows appear to be quite well insulated since they do not appear to be radiating much more than the center window, which was bricked over. The area of major heat loss in this photo is the attic vent located near the peak. Although it may not be desirable to seal it off completely because of moisture buildup in the attic, it may be possible to reduce its area without affecting its function as a vent. This photo displays the ease with which inadvertant draft type of heat losses can be recognized with the proper thermographic instrumentation.

Figure 4a is a front view of building 171. Note that in this picture the windows are warmer than those in Figure 3. The right side of the first floor appears cooler than the rest of the building. This is not due to the insulating quality of the walls but rather a result of those sections of the wall being ivy covered--as can be seen in the photograph. The walls themselves are probably at a relatively uniform temperature, while the cool thermal image of the ivy is approximately ambient. Attention is drawn to the belfry atop the building with its bright thermal image indicating a heat loss.

Figure 5a is a front view of headquarters building 151. An interesting point to note in this thermograph are the windows above the main entrance. Notice the difference in the upper and lower halves of the windows. The warm lower half and cool upper half indicates that either the lower half of the storm window is missing or else it was left open in the up position leaving a double storm window above and no storm window below.

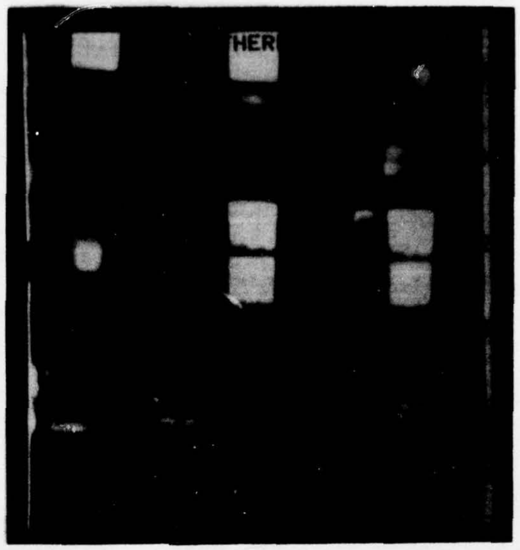

Fig 2a Thermogram of BOQ located on Navy Hill

Fig 2b Photo of BOQ

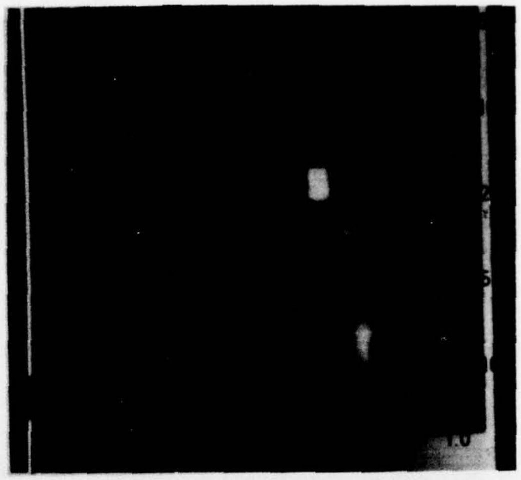

Fig 3a Thermogram of north end of building 183

Fig 3b Photo of north end of building 183

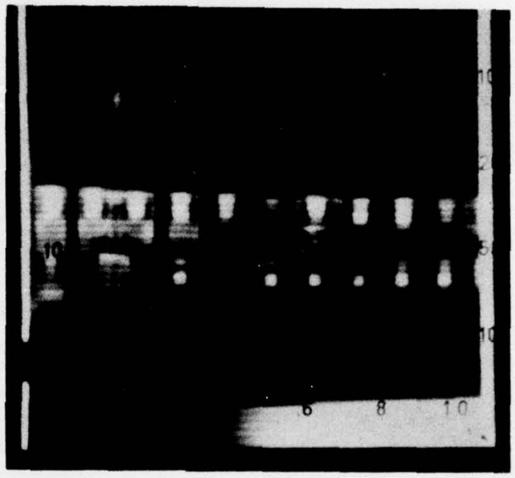

Fig 4a   Thermogram of front view of building 171

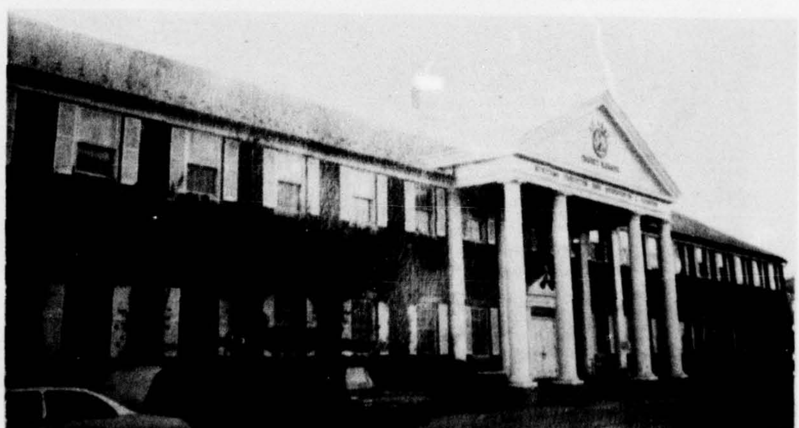

Fig 4b   Photo of building 171

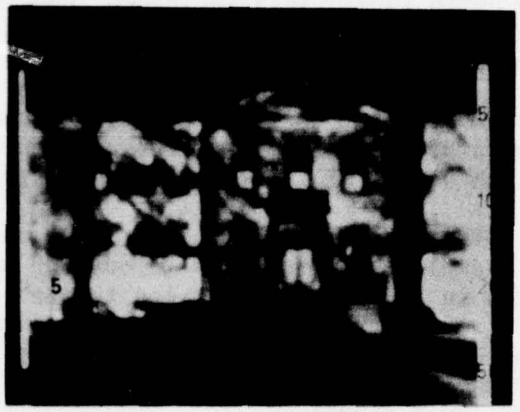

Fig 5a Thermogram of building 151

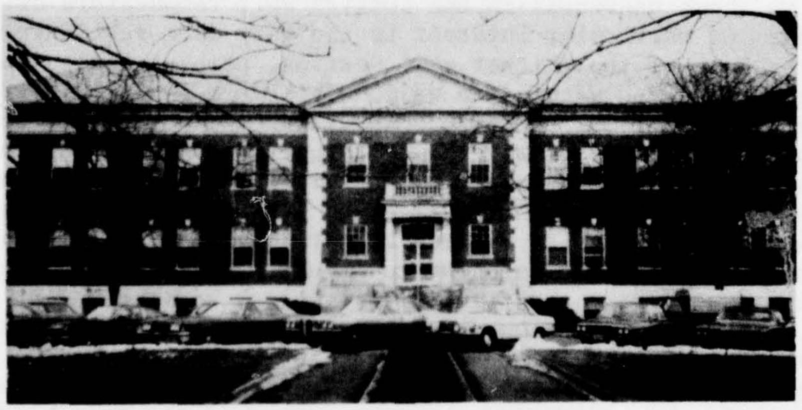

Fig 5b Photo of building 151

Figure 6a is a thermogram of the home next to building 59 showing heat leaks under the overhang along the roofline. It is interesting to note the high radiometric temperature along the inside corner above the porch roof. This increased temperature is probably a combination of heat loss and low wind velocity in the region of the inside corner causing a warm region of relatively stagnant air. Great care must be exercised in the interpretation of this type of thermograph in terms of heat loss because of the complicated interplay of air temperature, wall temperature, and convective and radiative exchange which occurs at inside corners of structures.

Figure 7a, a thermogram of the change house on the Navy Hill Road, is a good example of differences in outside wall temperature due to differences in thermal transmission through the wall. Notice the difference in radiometric temperature between the upper and lower half of the building. Either the insulating value of the wall is different, or the inside temperature of the building is different between upper and lower floors.

Figure 8a shows the rear side of Headquarters, building 151 thermographically. Notice the warmer horizontal and vertical areas where the floors and walls butt to the outside wall indicating a high thermal coupling the those regions. Again, notice the effect of double storm windows wherever there is an air conditioner requiring the partial opening of a window.

Figure 9 gives several thermographic views of building 10. Figure 9a shows uneveness in the outside wall temperature of the building. Of particular interest is the very warm region running along the base of the thicker wall section, perhaps indicating a steam pipe imbedded within the wall. This warm region is visible in all three thermograms. In Figure 9b we can see a large difference in outside wall temperature. We feel this is due to a wall mounted radiator located on the inside. The straight line on the left of the window is the outline of a tree and just to the left of it is a section of the wall which is much cooler than the warm region around the windows. Figure 9c is shown to illustrate the difference in the thermal properties of the tile building block and the cement mortar joints. The outside radiometric temperature of the blocks is cooler than the mortar joints since the air holes within the blocks act as an insulating layer. Using the isothermal scale built within the instrument, it was estimated that the center of the tile blocks outside surface are about 3°C above ambient while the mortar joints are about 4.5°C above ambient.

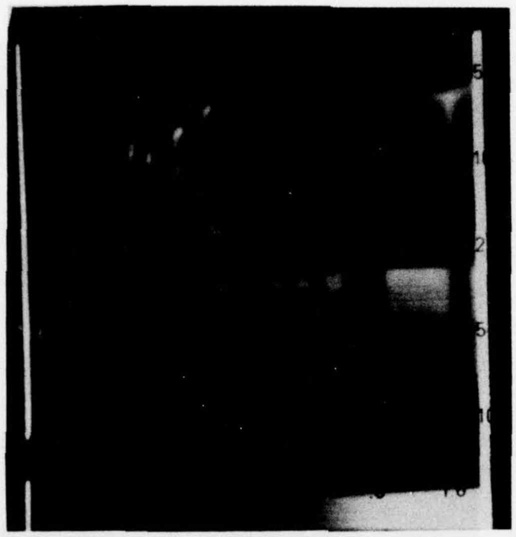

Fig 6a Thermogram of home next to building 59

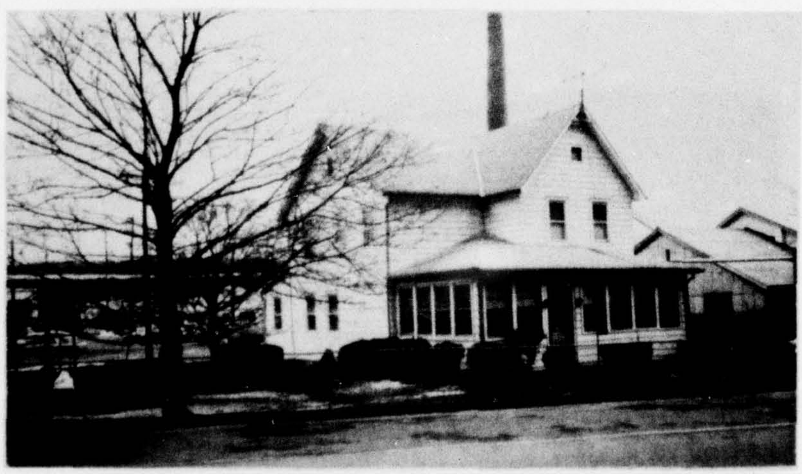

Fig 6b Photo of home next to building 59

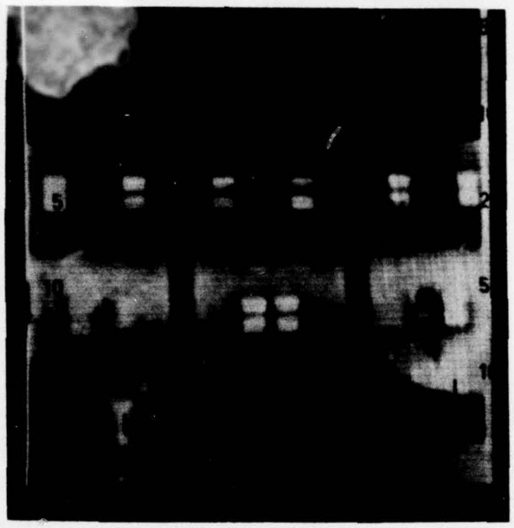

Fig 7a   Thermogram of changehouse on Navy Hill Road

Fig 7b   Photo of changehouse on Navy Hill Road

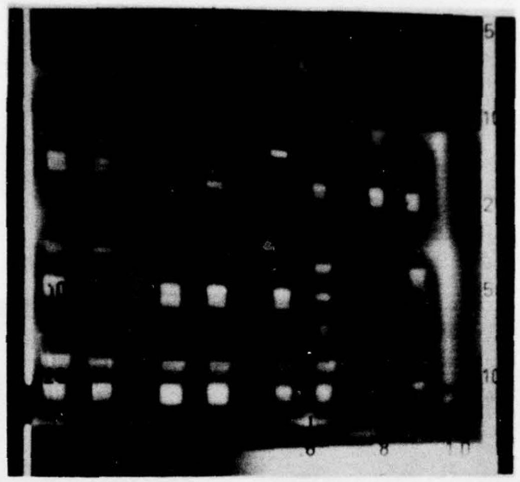

Fig 8a   Thermogram of backside of building 151

Fig 8b   Photo of backside of building 151

Fig 9a   Thermogram of building 10

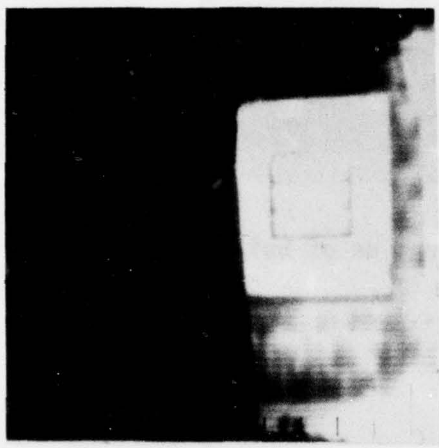

Fig 9b   Thermogram showing variation in outside wall temperature

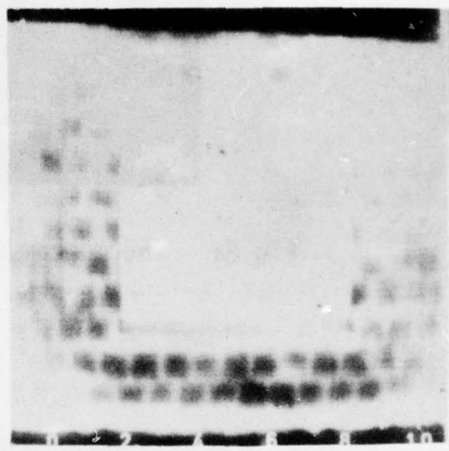

Fig 9c   Thermogram showing a variation in thermal properties of construction tile

Photo of building 10

Figure 10a is a thermogram of building 329 taken with an 8° field of view lens from the vantage point of Picatinny Peak. This illustrates what sort of information is possible from an aerial survey. Detailed resolution is obviously missing, however, this is a good way for spotting gross effects over a large area in a relatively short time. It is obvious, for instance, that the small annex is much warmer on the exterior than the main building. Also of interest are the two very warm windows on the near side of the main building which would warrant a physical inspection.

Figure 11a is a closeup view of a building illustrating detailed localized information in contrast to the information obtained in the aerial view of Figure 10. Notice the heat loss differences in the roof due to variations in the insulation. The parallel lines on the roof are due to the presence of roof rafters offering better thermal insulation than the area between the rafters. The noninsulated overhead door is also a source of thermal loss to the exterior.

Figure 12a shows a thermogram of building 307 indicating heat losses through the rectangular region in what was probably a skylight in the roof. This skylight is made of corrugated fiberglass and has since been painted over serving no useful purpose. It has no insulation whatsoever and can very well be the largest single heat loss in the building. Several of these regions are present on 307 and again the same situation exists on building 302 shown in Figure 12c.

Figure 13a is a thermographic view of the corridor connecting buildings 350 and 352 showing the poor thermal properties of this plastic covered structure.

Figure 14a is a thermographic recording of a section of steam line running up to Navy Hill. Notice that although the uninsulated valve is about 150°C above ambient, the outside temperature of the insulated pipe section is quite cool. It was noted during the course of this survey that different steam pipe sections had large variation in the insulation quality of the pipe wrapping. For example, in Figure 14c the valve in the 350 area is again about 150°C above ambient but in this case notice that the pipe wrapping has a higher temperature than the section shown in Figure 14a. Neglecting emmissivity, variations could indicate somewhat poorer insulation in this particular section of pipe. Figure 14d shows the ease with which poor insulation spots can be found on a steam line. By scanning the steam line from a vehicle, poor insulation regions show up as bright easily discernible areas as shown in the figure.

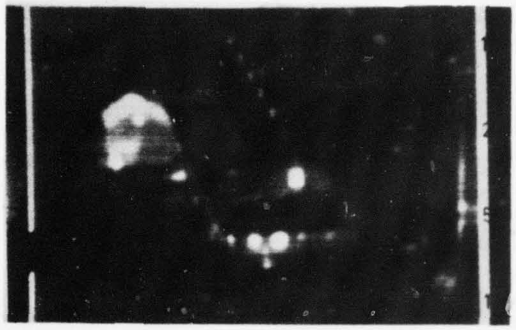

Fig 10a Thermogram of building 329 taken from Picatinny Peak

Fig 10b Photo of building 329

Fig 11 Thermogram of close-up view of building showing heat loss through roof

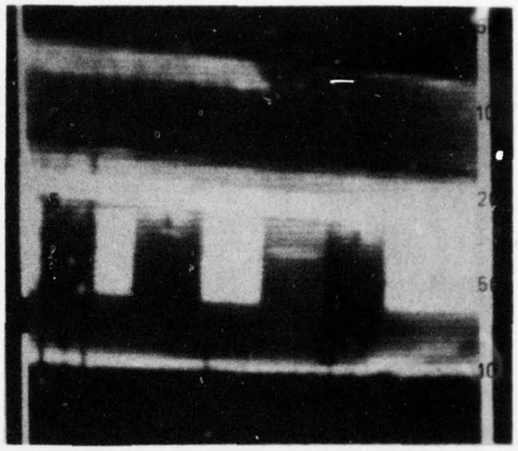

Fig 12a   Thermogram of building 307

Fig 12b   Photo of building 307

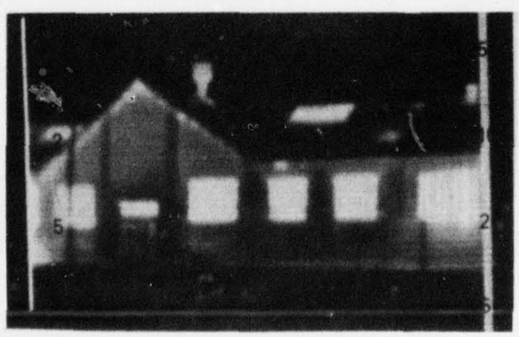

Fig 12c   Thermogram of building 302

Fig 13a Thermogram of corridor connecting buildings 350 and 352

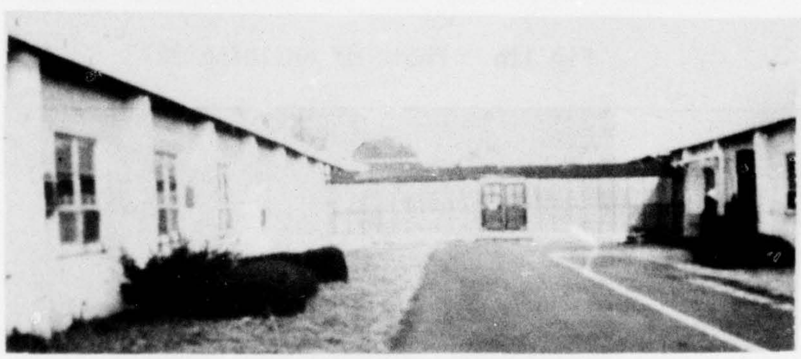

Fig 13b Photo of corridor connecting buildings 350 and 352

Fig 14a   Thermogram of steam pipe and valve (Navy Hill)

Fig 14b   Photo of steam pipe and valve

Fig 14c   Thermogram of steam pipe and valve (350 area)

Fig 14d   Thermogram showing poor circulation spot in steam line

Figure 15a shows a thermographic view of an electrical transformer and distribution box located behind building 95. In Figure 15a the transformer and distribution box are shown with the transformer somewhat warmer. Also shown in this thermogram is an overhead steam line with a valve and two uninsulated support points showing. The three high voltage connectors showing in Figure 15c do not have a thermographic signature in Figure 15a because they are very cool. In Figure 15b we have another thermographic view of the station with an isothermal contour set for slightly above ambient temperature. Notice the outline of the high voltage connectors indicating a very uniform temperature at slightly above ambient. A complete scan of this station through the isotherm range indicated no exceptionally hot region. The best time to examine such station would of course be during the daylight hours at a time when the station is at a peak load condition.

Figure 16a shows the north end of building 95 along with some elevated steam lines which show warm regions at each support point. This thermogram is included to show the effect of using the isothermal scan to determine temperature differences of relatively uniform thermographic image. Figure 16a shows the wall which yields a rather uniform heat picture except for the area around a vent. In Figure 16b, however, we have super-imposed an isothermal contour set at 4°C above ambient which we found to be the temperature of the warmest parts of the wall. Notice the detail visible in Figure 16b which indicates by bright areas all regions of the wall at 4°C above ambient which we found to be the temperature of the warmest parts of the wall. Notice the detail visible in Figure 16b which indicates by bright areas all regions of the wall at 4°C above ambient. It was found that the maximum temperature gradient of the wall was about 2°C from the warmest to the coldest.

Figure 17a is included to show the thermal losses from two ventilating fans left running all night at the officers club. A third fan to the left of the two warm ones was not running and so has a very dark thermal image.

Figure 18 shows a thermographic display of the 350 area as seen from the vantage point of Picatinny Peak. Figure 18a and 18b are the same thermographic views of the 350 area except that Figure 18b is a negative display (all cool areas appear bright and warm alreas are dark). Notice in Figure 18a how warm the 302 machine shop area appears in contrast to buildings 350 through 355. This warm area around 302 is largely a result of the roof of 302 being totally uninsulated and the walls contain many large windows. Notice also in Figure 18a the bright corridor connecting buildings 350 and 352 which was shown close up in Figure 13. It appears from Figure 18a

Fig 15a Thermogram of electrical station located behind building 95

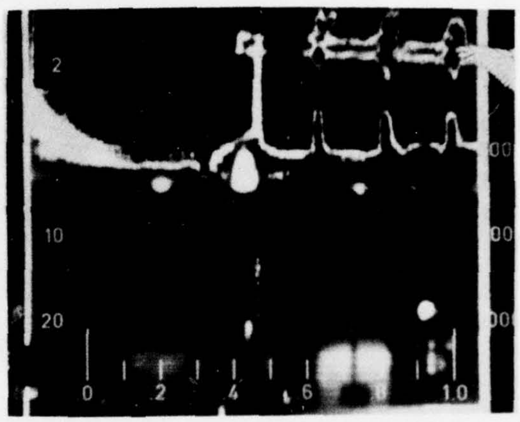

Fig 15b Thermogram of electrical station with isothermal contour

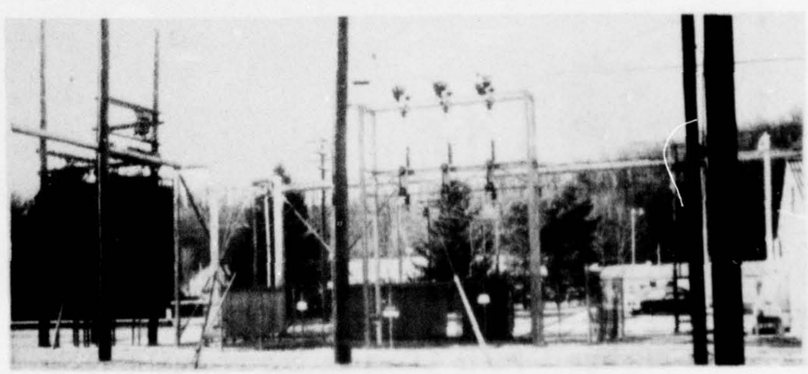

Fig 15c Photo of electrical station

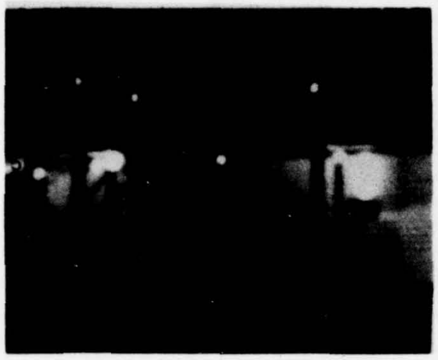

Fig 16a Thermogram of north end of building 95

Fig 16b Thermogram of north end of building 95 with isothermal contour set at 4°C above ambient

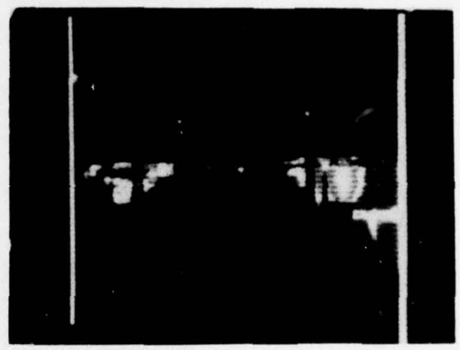

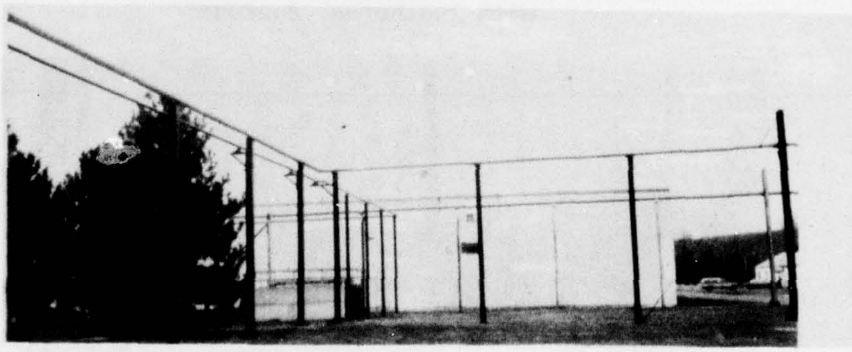

Fig 16c Photo of north end of building 95

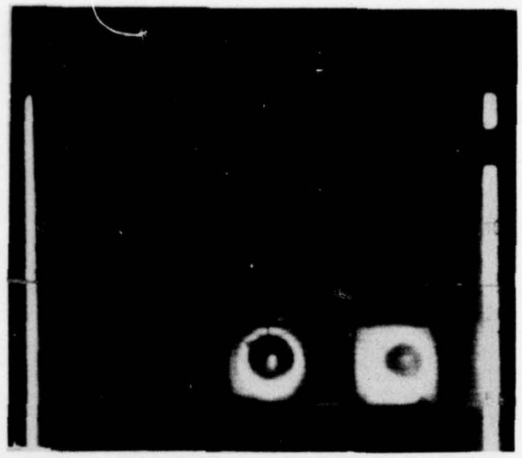

Fig 17a Thermogram of exhaust fans at Officers Club

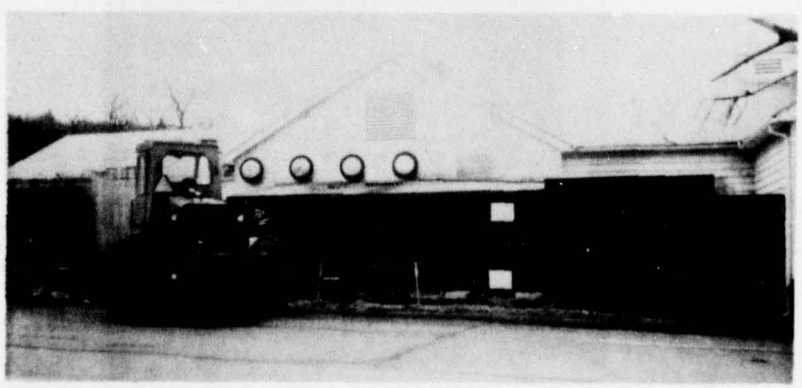

Fig 17b Photo of Officers Club

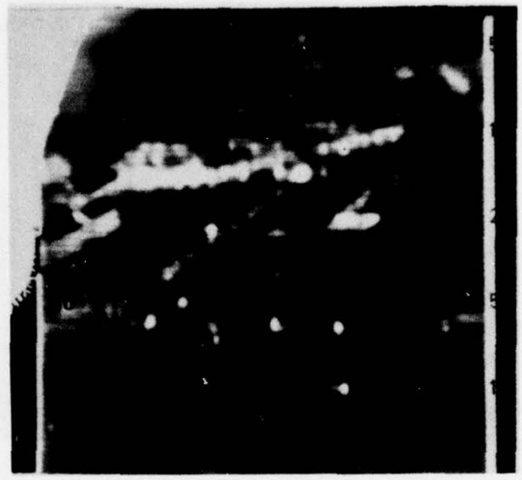

Fig 18a Thermogram of 350 area from Picatinny Peak

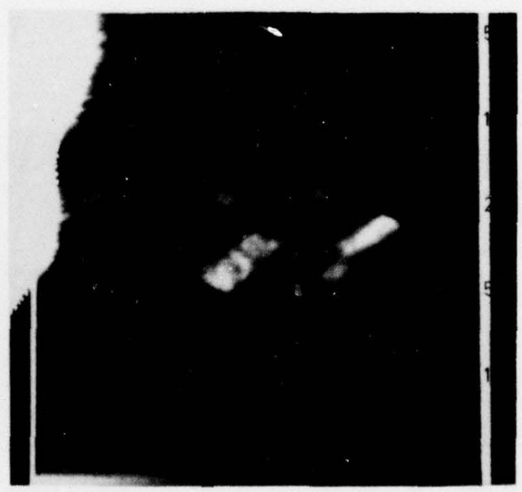

Fig 18b Inverted thermogram of 350 area
from Picatinny Peak

that the roofs of buildings 351 and 353 are darker and therefore radiometrically cooler than buildings 350, 352, 354, and 355. Again in the inverted picture (Fig 18b), notice how they appear brighter and therefore cooler than the others. Inasmuch as some of these roofs are metal and therefore of abnormally low emissivity, great caution must be exercised in inferring that these roofs are, in fact, cooler than their surroundings.

Figure 19 is a thermographic view of a section of the steam jacketed transport lines at the meltpour pilot facility being constructed at Picatinny. Variations in the effectiveness of the insulation are readily seen by the intensity variations of the thermographic image.

Figure 20 is included to illustrate another functional capability available for heat analysis. In order to get an immediate and quantitative comparison of the radiometric temperature of different points, a line is set through the picture region of interest. In this case, the line runs across a man's legs (seen on left) and through a live steam vent (next to the man). At the bottom of the display is a graphical representation of the radiometric signal at all points along the horizontal line. In this case, the steam vent being much hotter than the man, has gone off scale.

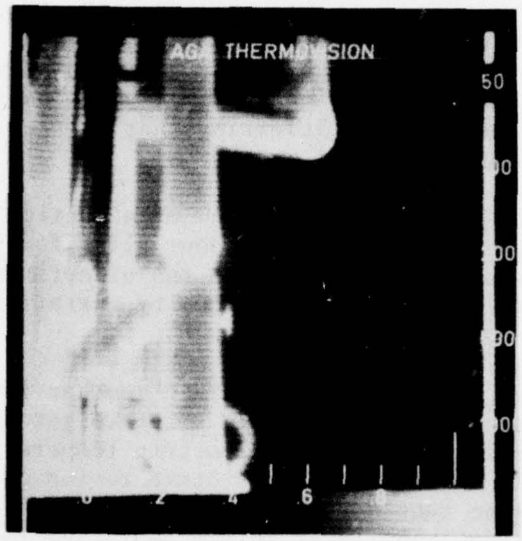

Fig 19 Thermogram of section of steam jacketed lines at melt pour pilot facility

Fig 20 Thermographic display with line scan giving quantitative comparison of radiometric temperature along that line

TECHNICAL DISCUSSION AND PROBLEM AREAS

The results from the typical thermograms discussed in this report point out many factors with which one must be concerned before thermographic imagery can be correctly interpreted. Two basic problems must be addressed. First, we must concern outselves with the correctness of the readings in terms of true temperature versus apparent, or radiometric temperature. Second, we must concern ourselves with interpreting true temperature measurements in terms of actual heat losses. Each of these is briefly discussed in the following.

True Temperatures vs Radiometric Temperature: Although a thermographic camera is sensitive to the radiation actually emanating from an object, it is also sensitive to any radiation which might be incident upon and reflected from the scene under study. Figure 21 shows the typical scenario in which thermograms are being made. As shown, one must be careful of the presence of intense background sources of IR. Failure to properly account for such factors will lead to serious errors when the data is interpreted. In the figure, for example, the sun constitutes a major source of IR illumination on the target. If one were interested in the temperature of the roof, he must consider at least three factors. First, the roof radiates its own contribution in accordance with its emissivity properties. Second, the roof reflects a portion of the solar IR illumination into the thermographic camera. This will be variable depending on such things as time of year and day, clarity of weather, reflectance of roof, specular or diffuse character of roof and/or illumination condition, etc. Third, the actual surface temperature of the roof is affected by the absoption of all external radiation impinging on it, by convective exchange with the outside air, by the internal temperatures of the building, and finally, by its own insulation quality. Because of the confusing effects of sunlight, it is best to take thermographic data of exterior surfaces after dark. This will reduce the variables we must contend with to those of object temperature, object emissivity, and background temperature.

As indicated earlier, the true temperature of a surface can be correctly inferred from the measured radiometric temperature only if emissivity and reflectance is properly accounted for. This relationship is symbolically illustrated in Figure 22. For example, special care must be taken when working with unpainted, metal surfaces. Since such surfaces have poor emissibity and high reflectivity, it is not unusual for the inexperienced thermographer to measure the thermal reflection from his own body and attribute this to the "temperature" of the metal. Conversely, slight emissivity variations over the surface due to dirt stains, uneven oxidation, etc can be

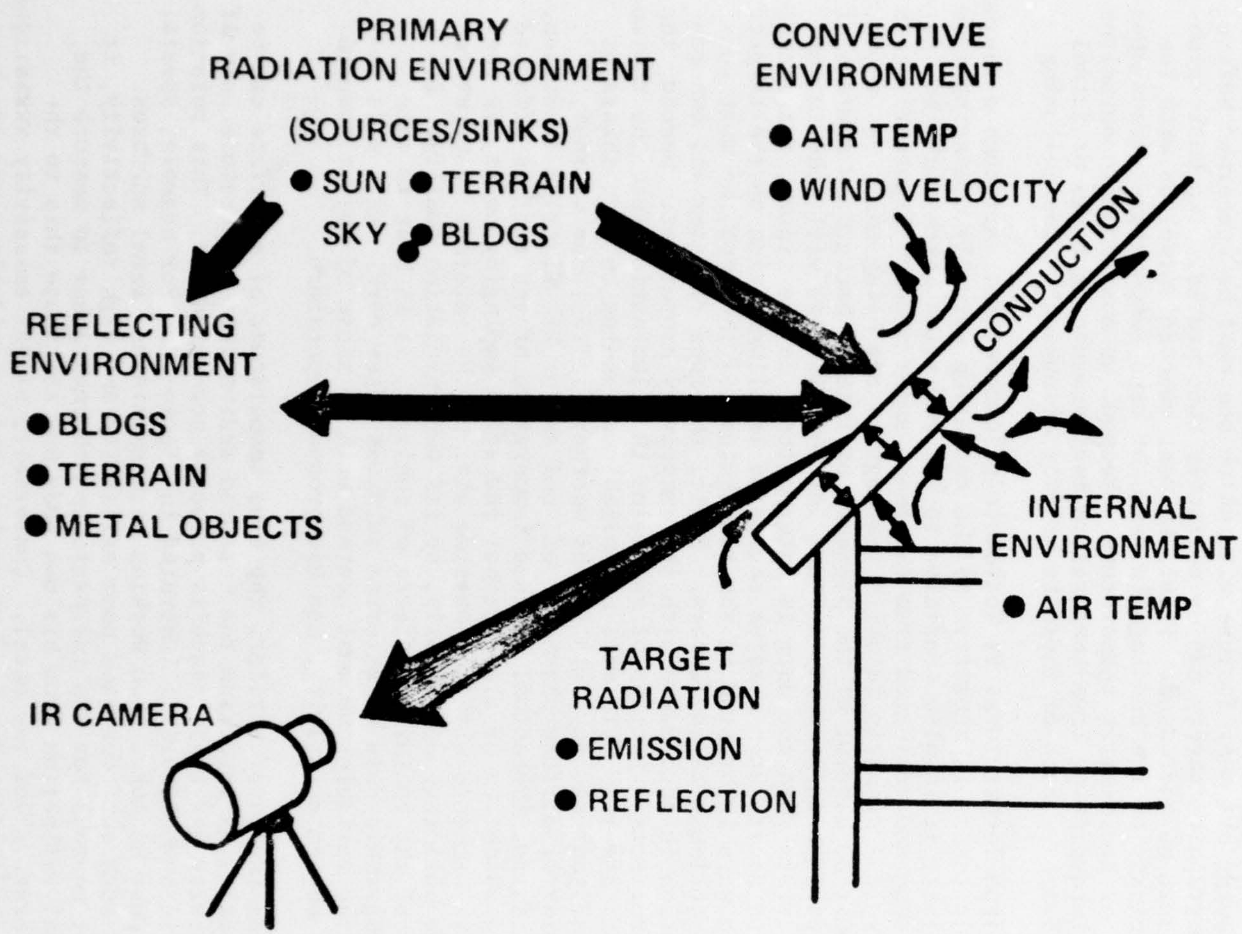

Fig 21 Thermographic environmental parameters

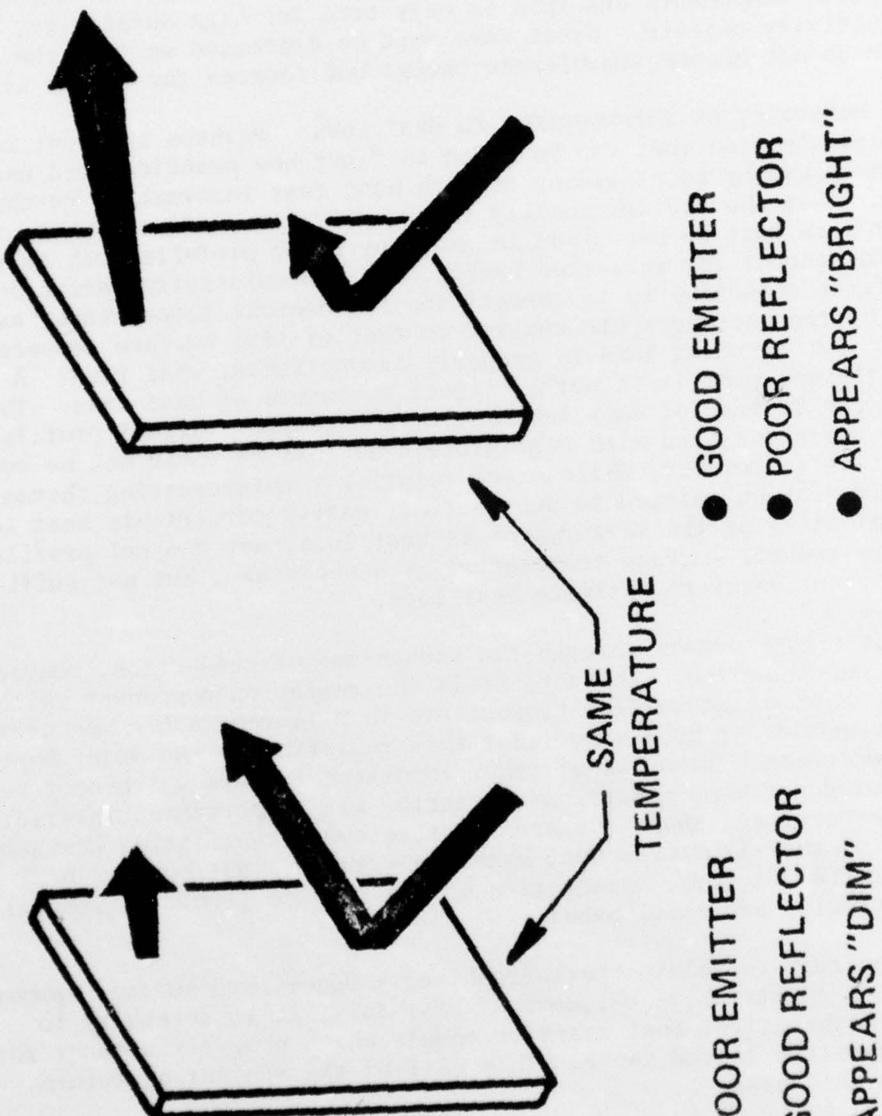

Fig 22 Emissivity

inferred as temperature variations even when the metal is uniformly isothermal. The situation would be further confounded if one is working in the presence of plant machinery and multiple reflections can occur. In most cases of qualitative thermography, it is assumed that particularly hot zones are radiating sufficiently to overshadow reflected components but this is only true for high emissivity, low reflectivity objects. Great care must be exercised so that the hot zones do not become troublesome background sources for nearby areas.

Relevancy of Thermography to Heat Loss: Perhaps the most important question that can be asked is "just how practical and useful is thermography in providing us with heat loss information to the extent that the savings justify the means." As mentioned above, great care must be exercised in avoiding major pitfalls such as failure to account for reflected backgrounds and emissivity variations. The first objective is to correct the radiometric temperature, as seen by the thermographic camera, to that of true surface temperature. But assuming this is properly accomplished, what then? A true thermal profile is not by itself a measure of heat loss. Thermograms can be made of many interesting and complex thermal profiles, which are associated with negligible heat loss or would not be cost-effective to correct, while other relatively uninteresting thermal profiles can be related to substantial, easily correctible heat loss. The objective of the measurement is heat loss, not thermal profile. In this report, surface temperature is a necessary, but not sufficient requirement to estimate heat loss.

Heat loss occurs through the mechanisms of conduction, convection, and radiation. In fact, it is the radiation component which allows us to infer surface temperature in a thermographic measurement but it should not be assumed that this radiation is the major heat loss mechanism. Examples of other important factors which must be considered are wind conditions, exterior air temperature, interior wall temperature, shape and area of structure, ventilation characteristics of the structure, heat exchange with adjacent bodies, heat inputs (i.e., solar), orientation of the surface (i.e., horizontal or vertical), and still others.

In order to relate thermographically determined surface temperature to a quantitative estimate of heat loss, it is necessary to employ mathematical heat transfer models which properly account for the parameters listed above. This will be the subject of future work in this area.

APPENDIX

PLANCK'S RADIATION LAW

The radiation emitted from a surface as a consequence of its temperature is given by Planck's Law:

$$W(\lambda) = \frac{\varepsilon(\lambda) 2\pi hc^2 \lambda^{-5} 10^{-6}}{e^{hc/\lambda kT} - 1} \text{ watts/m}^2\mu \quad (1)$$

where:

$W(\lambda)$ = the radiant emittance per unit wavelength band

C = velocity of light, 3×10^8 m/sec

h = Planck's constant, 6.6×10^{-34} joule-sec

k = Boltzmann's constant, 1.4×10^{-23} joule/°K

T = temperature of body, °K

λ = wavelength, microns

$\varepsilon(\lambda)$ = *surface emissivity as function of wavelength*

The total radiation from a surface is obtained by integrating the above over all wavelengths.

$$W = \int_0^\infty W(\lambda) d\lambda = \varepsilon\sigma T^4 \quad (2)$$

where:

ε = object emissivity (assumed constant) of body

σ = Stefan-Boltzmann constant, 5.7×10^{-8} watt/m^2-°K

A plot of equation (1) is given in Figure 23 and typically demonstrates the increase in radiation due to temperature at any particular wavelength.

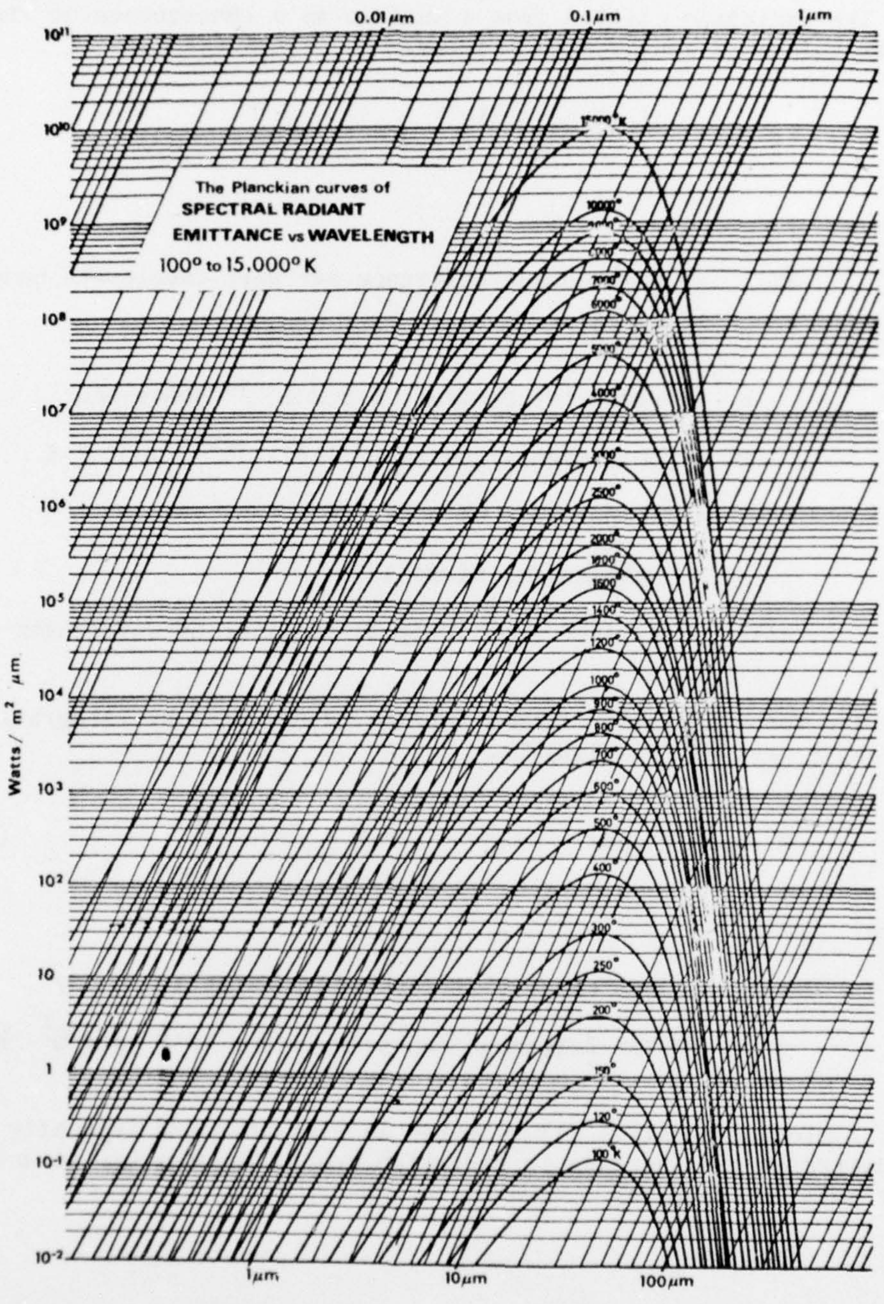

Fig 23 The Planckian curves of spectral radiant emittance vs wavelength 100° to 15,000°K

DISTRIBUTION LIST

	Copy No.
Commander US Army Materiel Development and Readiness Command ATTN: DRCQA DRCDE DRCDE-R DRCDL-CS 5001 Eisenhower Avenue Alexandria, VA 22301	1 2 3 4
Commander Production Equipment Agency ATTN: DRXIB-MT Rock Island, IL 61201	5
Commander US Army Research Office - Durham ATTN: Physics Division Electronics Division Materials Division Box CM, Duke Station Durham, NC 27706	6 7 8
Commander Harry Diamond Laboratories ATTN: Technical Library Washington, DC 20438	9
Commander Defense Documentation Center Cameron Station Alexandria, VA 22314	10-21
Commander US Army Foreign Science and Technology Center ATTN: DRXST-SD3 220 Seventh Street, NE Charlottesville, VA 22901	22
Office of Chief of Research and Development Department of the Army ATTN: DARD-ARS-P Washington, DC 20310	23

Commander
US Army Materiel Development and Readiness Command
ATTN: DRCQA-V 24
DRCQA-E 25
DRCQA-P 26
DRCDE-R 27
DRCDL 28
DRCDE-EA 29
DRCDE-U 30
Alexandria, VA 22304

Commander 31
US Army Electronics Command
Fort Monmouth, NJ 07703

Commander
US Army Missile Command
ATTN: AMSMI-RP, Redstone Scientific Information Center 32-34
Redstone Arsenal, AL 35809

Commander 35
US Army Troop Support Command
4300 Goodfellow Boulevard
St. Louis, MO 63120

Commander
US Army Natick Laboratories
ATTN: STSNLT-EQR 36
STSNLT-GE 37
Kansas Street
Natick, MA 01760

Commander
US Army Mobility Equipment Research
and Development Center
ATTN: STSFB-E 38
STSFB-M 39
STSFB-MM 40
STSFB-X 41
STSFB-D 42
STSFB-DQ 43
STSFB-O 44
STSFB-J 45
STSFB-W 46
Fort Belvoir, VA 22060

Director
USA Mobility Equipment Research and
  Development Center
Coating and Chemical Laboratory
ATTN: STSFB-CL 47
Aberdeen Proving Ground, MD 21005

Commander
US Army Tank-Automotive Command
ATTN: DRDTA 47
28251 Van Dyke Avenue
Warren, MI 48090

Commander
US Army Armament Materiel Readiness Command
ATTN: DRSAR-QA 48-49
DRSAR-SC 50
DRSAR-RDP 51
DRSAR-EN 52
Rock Island, IL 61201

Commander
US Army Aviation Systems Command
ATTN: DRSAV 53
St. Louis, MO 63166

Commander
US Army Aeronautical Depot Maintenance Center
(Mail Stop 55)
ATTN: DRSAD-FES, Mr. Bee 54
Corpus Christi, TX 78419

Commander
US Army Test and Evaluation Command
ATTN: DRSTE-RA 55
Aberdeen Proving Ground, MD 21005

Commander
US Army White Sands Missile Range
ATTN: STEWS-AD-L 56
STEWS-ID-P 57
Albuquerque, NM 88002

Commander
US Army Yuma Proving Ground
ATTN: STEYP-MTS 58
STEYP-ADT 59
Yuma, AZ 85364

Commander
US Army Tropic Test Center
ATTN: STETC-XO-A, Drawer 942 60
Ft Clayton, CZ

Commander
US Army Arctic Test Center
ATTN: STEAC-MO-AS 61
APO, Seattle 98733

Commander
Dugway Proving Ground
ATTN: STEPD-TO(D) 62
Utah 84022

Commander
US Army Electronic Proving Ground
ATTN: STEEP-MT 63
Ft Huachuca, AZ 85613

Commander
Jefferson Proving Ground
ATTN: STEJP-TD-1 64
Madison, IN 47250

President
US Army Airborne
Communications and Electronics Board
ATTN: STEBF-TD 65
Ft Bragg, NC 28307

President
US Army Air Defense Board
ATTN: STEBD-TD 66
Ft Bliss, TX 79916

President
US Army Armor and Engineer Board
ATTN: STEBB-TD 67
Ft Knox, KY 40121

President
US Army Aviation Test Board
ATTN: STEBG-MT 68
Ft Rucker, AL 36360

President
US Army Field Artillery Board
ATTN: STEBA-TD
Ft Sills, OK 73503 69

President
US Army Infantry Board
ATTN: STEBC-TE
Ft Benning, GA 31905 70

Commander
Anniston Army Depot
ATTN: DRXAN-QA
Anniston, AL 36202 71

Commander
Letterkenny Army Depot
ATTN: DRXLE-QA
Chambersburg, PA 17201 72

Commander
Lexington-Bluegrass Army Depot
ATTN: DRXLX-QA
Lexington, KY 40507 73

Commander
New Cumberland Army Depot
ATTN: DRXNC-QA
New Cumberland, PA 17070 74

Commander
Pueblo Army Depot
ATTN: DRXPU-Q
Pueblo, CO 81001 75

Commander
Red River Army Depot
ATTN: DRXRR-QA
Texarkana, TX 75501 76

Commander
Sacramento Army Depot
ATTN: DRXSA-QA
Sacramento, CA 95801 77

Commander
Savanna Army Depot
ATTN: DRXSV-QA
Savanna, IL 61074 78

Director
AMC Ammunition Center
ATTN: SARAC-D
Savanna, IL 61074 79

Commander
Seneca Army Depot
ATTN: DRXSE-RG
Romulus, NY 14541 80

Commander
Sharpe Army Depot
ATTN: DRXSH-QE
Lathrop, CA 95330 81

Commander
Sierra Army Depot
ATTN: DRXSI-DQA
Herlong, CA 96113 82

Commander
Tobyhanna Army Depot
ATTN: DRXSI-Q
Tobyhanna, PA 18466 83

Commander
Tooele Army Depot
ATTN: DRXTE-QA
Tooele, UT 84074 84

Chief
Bureau of Naval Weapons
Department of the Navy
Washington, DC 20390 85

Chief
Bureau of Ships
Department of the Navy
Washington, DC 20315 86

Naval Research Laboratory
ATTN: Dr. J. M. Krafft, Code 8430 87
Washington, DC 20375

Commander
US Army Armament Research and Development Command

ATTN:	DRDAR-LC, Col P. B. Kenyon	88
	DRDAR-LC, Dr. J. Frasier	89
	DRDAR-LC, Mr. J. Gregorits	90
	DRDAR-LC, Mr. E. Kelley	91
	DRDAR-LC, Mr. S. Jacobson	92
	DRDAR-LCV, Mr. F. Youngblood	93
	DRDAR-LCP, Mr. W. Kauf	94
	DRDAR-LCA, Dr. E. Sharkoff	95
	DRDAR-LCE, Dr. R. Walker	96
	DRDAR-LCM, Mr. L. Saffian	97
	DRDAR-LCM-SE, Mr. John Swatinsky	98
	DRDAR-LCS, Mr. E. Vaughan	99
	DRDAR-LCS, Mr. R. Allen	100
	DRDAR-LCW, Mr. H. Garren	101
	DRDAR-LCW, Mr. W. Pape	102
	DRDAR-LCB, Mr. P. Rummel	103
	DRDAR-LCB, Mr. R. Allen	104
	DRDAR-LCF, Mr. F. Saxe	105
	DRDAR-LCN, Col G. Lubold, Jr.	106
	DRDAR-LCU, Mr. A. Moss	107
	DRDAR-LCP-OP, Mr. W. Powers	108
	DRDAR-LCU-D, Mr. G. Jackman	109
	DRDAR-PBM, Mr. H. W. Painter	110
	DRDAR-PC, Mr. F. Santucci	111
	DRDAR-TDS, Mr. V. Lindner	112
	DRDAR-LCA, Mr. T. Strano	113
	DRDAR-LCA, Mr. C. Cavanaugh	114
	DRDAR-QA-S, Mr. J. Gold	115
	DRDAR-QAN, Mr. P. Olivieri	116
	DRDAR-LCP, PD, Mr. W. Doremus	117-118
	DRDAR-LCP, PP, Mr. P. Kisatsky	119-122
	DRDAR-LCP-PP, Mr. M. Barbarisi	123-126
	DRDAR-LCP-PL, Mr. G. G. Tirellis	127-130
	DRDAR-LCN-F, Dr. Len Nichols	131
	DRDAR-LCP-PL, Mr. J. Costantino	132
	DRDAR-LCP-PP, Mr. J. W. McGarney	133
	DRDAR-LCM-P, Mr. P. Quatrochi	134
	DRCPM-PBM, General J. Egbert	135
	DRCPM-PBM-GB, Mr. John Gehbauer	136
	DRDAR-TDR, Dr. R. Eichelberger	137
	DRDAR-TDA, Mr. J. Blich	138
	DRDAR-TSS	139-143

Dover, NJ 07801